Efficient quantitative assessment of robot swarms: coverage and targeting Lévy strategies

Siobhan Duncan*, Gissell Estrada-Rodriguez*, Jakub Stocek*, Mauro Dragone, Patricia A. Vargas, Heiko Gimperlein

***Abstract*—Biologically inspired *strategies* have long been adapted to swarm robotic systems, including biased random walks, reaction to chemotactic cues and long-range coordination. In this paper we show the opportunities provided by *analysis tools* developed for biological systems, such as continuum models, for the efficient quantitative characterization of robot swarms. These tools lead to fast methods for the optimization of robot movement laws to achieve a prescribed collective behavior. We show how to compute performance metrics like coverage and hitting times, and illustrate the accuracy and efficiency of our approach for area coverage and search problems. Both Brownian and Lévy strategies with a characteristic long-range movement are discussed. Comparisons between the continuum model and robotic simulations confirm the quantitative agreement and speed up by a factor of over 100 of our approach. Results confirm and quantify the advantage of Lévy strategies over Brownian motion for search and area coverage problems in swarm robotics.**

***Index Terms*—Swarm robotics, multi-agent systems, diffusion equation, optimization, coverage, target search, Lévy walks.**

I. Introduction

Swarm robotics can be formally defined as "the study of how a large number of relatively simple physically embodied agents can be designed, such that a desired collective global behaviour emerges from the local interactions among the agents and between the agents and the environment" [44].

Insect societies and bird flocks provide compelling examples of optimal global behaviour patterns emerging from the interaction of simple agents without the intervention of complex reasoning and centralised supervision. In contrast, they demonstrate systems with strong self-organizational and emergent properties that are able to organize their activities and achieve tasks with exceptional robustness. These properties make biologically inspired approaches [10], [16] quite appealing for robot swarms in search and coverage applications, for instance, in rescuing operations in disaster regions [20], foraging for natural resources [23], exploration/mapping [33], environmental monitoring [45], cooperative cleaning [4], and in surveillance scenarios [21].

Multiple robots can spread across an environment in order to sense it from different vantage points and distribute themselves to maximize the rate at which the environment is explored. Since robots do not need to build shared models of their environment, nor globally agreed plans, biologically-inspired robot swarms can be more robust and fault tolerant, and potentially more scalable and more suitable to unknown and dynamic environments than centralised coordination approaches [43].

However, all this flexibility comes at a price. Crucially, the biggest hurdle for applying swarm robotic approaches is the inherent difficulty in engineering the behaviour of each robot to achieve system-level properties [7]. Behavior-based, bottom-up design is the most common approach to develop a swarm robotics system [42]. Control laws for individual robots' behaviours are implemented and successively improved, usually by relying on soft-computing methods such as multi-robot reinforcement-learning [34] and evolutionary algorithms used in evolutionary robotics [38], [51], until the overall swarm exhibits the desired global behaviour. Simulations are often necessary, as these methods require many iterations to converge and it would be simply unpractical and take an extremely long time to run numerous field tests with many real robots. Although simulations are much faster than real experiments, the results of simulations are not easily generalized [11]. In addition, they usually do not scale well, for the greater the number of robots to be simulated, the longer it takes to obtain results. Consequently, the development of robotic swarms is usually limited to specific scenarios where both tasks and environment are strictly defined. Hence, it is hard to provide and predict the effect of changes either in each robot's behaviour, or in the number of robots in the overall swarm performance.

We tackle these problems using tools developed for the modelling of biological systems. We start from the movement of the individual robot, including local communication and interactions. As an example, we derive a continuum model for Brownian and Lévy [22] strategies with characteristic long-range movements. This is then used for the efficient quantitative characterization of robot swarms in search and area coverage applications. The resulting continuum models describe the evolution of the probability density of robots in terms of a non-local macroscopic diffusion equation. They not only allow fast computational approaches, but also provide analytical insights into the system-level behaviour of the robot collective [39].

*These authors contributed equally to this article.

Maxwell Institute for Mathematical Sciences and Department of Mathematics, Heriot–Watt University, Edinburgh, EH14 4AS, United Kingdom.

Institute for Mathematics, University of Paderborn, Warburger Str. 100, 33098 Paderborn, Germany.

Robotics Lab, Edinburgh Centre for Robotics, School of Mathematical and Computer Sciences and School of Engineering and Physical Sciences, Heriot–Watt University, Edinburgh, EH14 4AS, United Kingdom.

H. G. acknowledges support by ERC Advanced Grant HARG 268105. G. E. R. and J. S. were supported by The Maxwell Institute Graduate School in Analysis and its Applications, a Centre for Doctoral Training funded by the UK Engineering and Physical Sciences Research Council (grant EP/L016508/01), the Scottish Funding Council, Heriot-Watt University and the University of Edinburgh.

Our results show that area coverage and hitting times can be computed from the macroscopic robot density. The experiments illustrate quantitative agreement for these quantities with individual robot simulations within the statistical margins of error, at a fraction of the computational cost. The results also confirm the advantage of anomalous diffusion strategies. For instance, both analytical and numerical results show a matching exponential increase of the hitting time with the Lévy exponent. Moreover, our numerical implementation provides a fast method to predict the global performance of a swarm robotic system and optimize individual robot movement laws to achieve a desired collective behavior.

This paper shows the insights and methods which can be obtained by adapting ideas from continuum models of interacting particle systems to robotic problems. Detailed models for concrete applications will be pursued elsewhere.

The remainder of the paper is organised as follows: Section II provides an overview of related work. Section III introduces the search strategy, while Section IV states the macroscopic description and how it is used to compute coverage and hitting times. The proof of the macroscopic description is the content of Section V. Section VI describes the robotic simulations and Section VII the numerical approach. These are compared in Section VIII. Section IX summarises our conclusions.

II. Related work

Simple approaches such as bacterial chemotaxis, phototaxis and run-and-tumble processes have been applied to individual robots [40]. For searching large areas for sparse and randomly located targets, a combination of biased random walk and Lévy strategies has proven to be efficient and robust to changes in the environment, for instance, in the case of underwater multi-robot systems [47].

From a different perspective, in swarm robotic systems Lévy strategies have also proven to be effective and provide a controlled model system to understand biological behavior. These strategies involve long-range movement, mimicking the behavior of T cells [29]. They prove useful for target search problems for sparsely distributed targets. Further examples where bio-inspired search strategies have been applied to robots include [14], [50].

For biological systems like flocks of birds or fish schools, self-organization and pattern formation have motivated the development of mathematical models to reproduce and analyze the collective behavior. An influential mathematical model governing these interacting particle systems was proposed by T. Vicsek et al. [52] in 1995. In this model, particles move with a constant speed and at each time step they align their velocity to the average velocity of the neighboring particles with some random perturbation. Subsequent works like [12] and [13] added realistic refinements to the mathematical description.

In the case of swarm robotic systems, some first macroscopic mathematical models have been studied in [5], [53]. The focus of their work is towards realistic metrics to measure the performance of a swarm robotic system, as a basis for its optimization and control. Only non-interacting Brownian robots are studied as the simplest possible model systems. Our work initiates the modeling of realistic robot movement by macroscopic partial differential equation (PDE) descriptions, as well as the specific performance metrics of coverage and hitting times, as relevant for the design of interactions and movement laws.

III. Description of the search strategy

A swarm robotics system consists of a large number of simple independent robots with local rules, communication and interactions among them and with the environment, where the local interactions may lead to collective behaviour of the swarm. In this work, we use a swarm of *e-puck* robots [37] in a domain in $\mathbb{R}^2$, which provides a specific model system. More generally, we consider N identical spherical individuals of diameter $\varrho > 0$ in $\mathbb{R}^n$, where $n = 2, 3$. Each individual is characterized by its position $\mathbf{x}_i \in \mathbb{R}^n$ and direction $\theta_i \in S = \{|\mathbf{x}_i| = 1\} \subseteq \mathbb{R}^n$. We assume that each individual moves according to the following rules:

1) Starting at position $\mathbf{x}$ at time t, an individual runs in direction θ for a Lévy distributed time τ, called the "run time".
2) The individuals move according to a velocity jump process with constant forward speed c, following a straight line motion interrupted by reorientation.
3) Each time the individual stops it selects a new direction θ^* according to a distribution $k(\mathbf{x}, t, \theta; \theta^*)$ which only depends on $|\theta - \eta|$.
4) When two individuals get close to each other they reflect elastically; the new direction is $\theta' = \theta - 2(\theta \cdot \nu)\nu$, where $\nu = \frac{\mathbf{x}_i - \mathbf{x}_j}{|\mathbf{x}_i - \mathbf{x}_j|}$ is the normal vector at the point of collision.
5) All reorientations are assumed to be instantaneous.
6) The running[1] probability ψ, which is defined as the probability that an individual moving in some fixed direction does not stop until time τ, is taken to be independent on the environment surrounding the individual.

Note that the assumptions correspond to independent individuals with simple capabilities relative to typical tasks for swarm robotic systems. They interact only with their neighbors in a narrow sensing region, and the movement decisions are based on the current positions and velocities, not information from earlier interactions. This assures the scalability to large numbers of robots, while non-local collective movement may emerge from local rules [46].

Related movement laws have been used for target search, for example, in the experiments in [29]. Refined local control laws and the possibility for quantitative experiments with robots open up novel modeling opportunities. In Section VIII we apply our results and present numerical experiments.

IV. Macroscopic description of robot coverage

The macroscopic model for the movement of interacting robots described in Section III is given, in the limit, by the following theorem.

[1]In probability theory this is also known as survival probability, where the "event" in this case is to stop. Hence "survival" in that context refers to the probability of continuing to move in the same direction for some time τ.

Theorem 1. *As $\varepsilon \to 0$, the macroscopic density $u(\mathbf{x},t)$ satisfy the following fractional diffusion equation:*

$$\partial_t u = c_0 \nabla \cdot \left(\frac{1}{F(u)}\ C_\alpha \nabla^{\alpha-1} u \right) \tag{1}$$

$$F(u) = \frac{\alpha-1}{\varsigma_0 |S|}(1-\nu_1) + \frac{32 c_0^3}{3|S|^2} u, \tag{2}$$

$$C_\alpha = -\frac{\varsigma_0^{\alpha-2} c_0^{\alpha-1} (\alpha-1)^2 \pi}{\sin(\pi\alpha)\Gamma(\alpha)} \frac{(|S|-4\nu_1)}{|S|^2}\ . \tag{3}$$

The term $F(u)$ comes from the interactions and C_α is the diffusion coefficient. The microscopic quantities in (2) and (3) are defined later in Section V, where ν_1 is the first non-zero eigenvalue of the turn angle operator T defined in (8).

To measure the coverage of the domain in the continuum sense, and be able to compare it with the discrete robotic simulations we define the following time averaged coverage function, used later in Section VIII, as

$$\mathrm{Cov}(t) = \frac{1}{t}\int_0^t \int_\Omega \min(u(\mathbf{x},s), \bar{\rho}) d\mathbf{x} ds \quad \text{where} \quad \bar{\rho} = \frac{1}{|\Omega|}\ . \tag{4}$$

The second quantity of interest that we compare with the webots simulations is hitting times. We seek the time t_0 at which the density of the solution at the target position T, reaches certain threshold δ, i.e.,

$$\delta = \int_{\mathsf{T}} u(\mathbf{x}, t_0) d\mathbf{x}\ ,$$

where T is the target position. In Section VIII we use an analytic expression for the solution u in $\mathbb{R}^n$ obtained in [27] as well as a numerical solution.

V. Microscopic description for individual movement

For the N-individual system described in Section III, the density $\sigma = \sigma(\mathbf{x}_i, t, \theta_i, \tau_i)$ evolves according to a kinetic equation [32]

$$\partial_t \sigma + c \sum_{i=1}^N \left(\partial_{\tau_i} + \theta_i \cdot \nabla_{\mathbf{x}_i}\right) \sigma = -\sum_{i=1}^N \beta_i \sigma\ . \tag{5}$$

The stopping frequency β_i during a run phase relates to the probability ψ_i that an individual does not stop for a time τ_i. It is given by

$$\psi_i(\mathbf{x}_i, \tau_i) = \left(\frac{\varsigma_0}{\varsigma_0 + \tau_i}\right)^\alpha,\ \alpha \in (1,2)\ . \tag{6}$$

This power law behaviour corresponds to the long tailed distribution of run times described in Assumption 1. in Section III, instead of the Poisson process in classical velocity jump models [41]. As the speed c of the runs is constant, the individuals perform occasional long jumps with a power-law distribution of run lengths. The stopping frequency is given by

$$\beta_i(\mathbf{x}_i, \tau_i) = -\frac{\partial_{\tau_i}\psi_i}{\psi_i} = \frac{\varphi_i}{\psi_i}\ . \tag{7}$$

After stopping, according to Assumption 3. individuals choose a new direction of motion according to the turning kernel T_i given by

$$T_i \phi(\theta_i^*) = \int_S k(\mathbf{x}_i, t, \theta_i; \theta_i^*) \phi(\theta_i) d\theta_i\ , \tag{8}$$

where the new direction θ_i^* is symmetrically distributed with respect to the previous direction θ_i according to the distribution $k(\mathbf{x}_i, t, \theta_i; \theta_i^*) = \tilde{k}(\mathbf{x}_i, t, |\theta_i^* - \theta_i|)$ [3].

A. Transport equation for the two-particle density

The description (5) of the N-particle problem a priori requires the understanding of collisions among the whole system of particles. In this section, however, we aim for a macroscopic description for low densities, as made precise by the scaling in Section V-B. In this case collisions of more than two individuals may be neglected [8], and we truncate the hierarchy of equations by neglecting collisions of 3 or more individuals and integrate out individuals $3, ..., N$ from σ. The transport equation which describes the movement of two particles is given by

$$\begin{aligned}\partial_{\tau_1}\sigma + \partial_{\tau_2}\sigma + \partial_t \sigma + c\theta_1 \cdot \nabla_{\mathbf{x}_1}\sigma + c\theta_2 \cdot \nabla_{\mathbf{x}_2}\sigma \\ = -(\beta_1 + \beta_2)\sigma\ ,\end{aligned} \tag{9}$$

where $\sigma = \sigma(\mathbf{x}_1, \mathbf{x}_2, t, \theta_1, \theta_2, \tau_1, \tau_2)$ is the two-particle density function and where $\sigma(\mathbf{x}_1, \mathbf{x}_2, 0, \theta_1, \theta_2, \tau_1, \tau_2) = \sigma_0(\mathbf{x}_1^0, \mathbf{x}_2^0, 0, \theta_1^0, \theta_2^0, \tau_1^0, \tau_2^0)$.

After stopping with rate given by β_1, particle 1 starts a new run at $\tau_1 = 0$ which is described by

$$\begin{aligned}&\tilde{\sigma}_{\tau_1}\big|_{\tau_1=0}(\mathbf{x}_1, \mathbf{x}_2, t, 0, \theta_1, \theta_2) \\ &\quad = \int_S k(\mathbf{x}_1, t, \theta_1^*; \theta_1) \int_0^t \beta_1 \tilde{\sigma}_{\tau_1}(\mathbf{x}_1, \mathbf{x}_2, t, \theta_1^*, \theta_2, \tau_1) d\tau_1 d\theta_1^* \\ &\quad = T_1 \int_0^t \beta_1 \tilde{\sigma}_{\tau_1}(\mathbf{x}_1, \mathbf{x}_2, t, \theta_1, \theta_2, \tau_1) d\tau_1\end{aligned} \tag{10}$$

and similarly for $\tilde{\sigma}_{\tau_2}\big|_{\tau_2=0}$, where $\tilde{\sigma}_{\tau_1}(\mathbf{x}_1, \mathbf{x}_2, t, \theta_1, \theta_2, \tau_1) = \int_0^t \sigma d\tau_2$.

Integrating (9) with respect to τ_1 and τ_2 and rewriting the terms $\int_0^t \beta_1 \tilde{\sigma}_{\tau_1} d\tau_1$ and $\int_0^t \beta_2 \tilde{\sigma}_{\tau_2} d\tau_2$ in (10) as in [26] we obtain

$$\begin{aligned}\partial_t \tilde{\tilde{\sigma}} + c\theta_1 \cdot \nabla_{\mathbf{x}_1}\tilde{\tilde{\sigma}} + c\theta_2 \cdot \nabla_{\mathbf{x}_2}\tilde{\tilde{\sigma}} \\ = -(\mathbb{1} - T_1) i_1(\mathbf{x}_1, \mathbf{x}_2, t, \theta_1, \theta_2) \\ - (\mathbb{1} - T_2) i_2(\mathbf{x}_1, \mathbf{x}_2, t, \theta_1, \theta_2)\ .\end{aligned} \tag{11}$$

Here the new density $\tilde{\tilde{\sigma}}(\mathbf{x}_1, \mathbf{x}_2, t, \theta_1, \theta_2) = \int_0^t \int_0^t \sigma d\tau_1 d\tau_2$ and

$$\begin{aligned}&i_1(\mathbf{x}_1, \mathbf{x}_2, t, \theta_1, \theta_2) \\ &\quad = \int_0^t \mathcal{B}_1 \tilde{\tilde{\sigma}}(\mathbf{x}_1 - c\theta_1(t-s), \mathbf{x}_2 - c\theta_2(t-s), s, \theta_1, \theta_2) ds\ , \\ &i_2(\mathbf{x}_1, \mathbf{x}_2, t, \theta_1, \theta_2) \\ &\quad = \int_0^t \mathcal{B}_2 \tilde{\tilde{\sigma}}(\mathbf{x}_1 - c\theta_1(t-s), \mathbf{x}_2 - c\theta_2(t-s), s, \theta_1, \theta_2) ds\ .\end{aligned} \tag{12}$$

The operator $\mathcal{B}$ describes the long-range movement of the particles given by the Lévy walk and is defined in terms of its Laplace transform as in [26], where $\mathcal{B}_1 = \mathcal{B}(\mathbf{x}_1, t-s)$ and $\mathcal{B}_2 = \mathcal{B}(\mathbf{x}_2, t-s)$.

B. Parabolic scaling

In applications, the mean run time $\bar{\tau}$ is often small compared with the macroscopic time scale $\mathcal{T}$, and we aim to study (11) for $\varepsilon = \bar{\tau}/\mathcal{T} \ll 1$ [3]. We introduce normalized variables t_n, x_n, τ_n, and c_n and a diffusion limit of (11) is obtained under the scaling $(\mathbf{x}, t, \tau) \mapsto (\mathbf{x}_n s/\varepsilon,\, t_n/\varepsilon,\, \tau_n/\varepsilon^{\mu})$, with $c_n = \varepsilon^{-\gamma} c_0$ for $\mu,\ \gamma > 0$. We further assume that the diameter of each robot is small, $\varrho = \varepsilon^{\xi}$, while the number of robots N is large so that $(N-1)\varrho = \varepsilon^{\xi-\vartheta}$, with $\xi - \vartheta < 0$.

C. PDE model for interacting robots with Lévy strategies

In the above parabolic scaling, this section obtains a fractional diffusion equation from (11) for the macroscopic density of robots moving according to the model in Section III.

First, from the two-particle density equation (11) we aim to derive a transport equation for the one-particle density function

$$p(\mathbf{x}_1, t, \theta_1) = \frac{1}{|S|} \int_0^t \int_0^t \int_{\Omega_2} \int_S \sigma d\theta_2 d\mathbf{x}_2 d\tau_1 d\tau_2 \ . \qquad (13)$$

This was done in [26] for the case of a system of interacting particles with long-range diffusion and alignment. Here we proceed similarly, so by integrating (11) with respect to the accessible phase space $(\mathbf{x}_2, \theta_2) \in \Omega_2 \times S$, where $\Omega_2 = \Omega_2(\mathbf{x}_1) = \{\mathbf{x}_2 \in \mathbb{R}^2 : |\mathbf{x}_1 - \mathbf{x}_2| > \varrho\} = \mathbb{R}^2 \setminus B_\varrho(\mathbf{x}_1)$ and introducing the scaling in Section V-B we obtain

$$\varepsilon \partial_t p + \varepsilon^{1-\gamma} c_0 \theta_1 \cdot \nabla p = \underbrace{\varepsilon^{-\gamma} \frac{c_0}{|S|} \int_{\partial B_\varrho} \int_S \nu \cdot (\theta_1 - \theta_2) \tilde{\tilde{\sigma}} d\theta_2 d\mathbf{x}_2}_{\text{(I)}}$$
$$\underbrace{- (\mathbb{1} - T_1) \int_0^t \mathcal{B}_1^{\varepsilon}(\mathbf{x}_1, t-s) p(\mathbf{x}_1 - c\theta_1(t-s), s, \theta_1) ds}_{\text{(II)}} \ . \qquad (14)$$

The first term in the right hand side of (14) comes from integrating $c\theta_1 \cdot \nabla_{\mathbf{x}_1}$ and $c\theta_2 \cdot \nabla_{\mathbf{x}_2}$ with respect to $\mathbf{x}_2$ and θ_2 and applying Reynolds' transport theorem in the variable $\mathbf{x}_2$. Since T is normalized, then from (11) the term $\int_{\Omega_2} \int_S (\mathbb{1} - T_2) i_2(\mathbf{x}_2, \mathbf{x}_1, t, \theta_1, \theta_2) d\theta_2 d\mathbf{x}_2 = 0$, and finally, the last term in (14) is obtained after changing the order of integration.

Up to lower order terms, we expand $p(\mathbf{x}_1, t, \theta_1)$ as follows

$$p(\mathbf{x}_1, t, \theta_1) = |S|^{-1} (u(\mathbf{x}_1, t) + \varepsilon^{\gamma} 2\theta_1 \cdot w(\mathbf{x}_1, t) + o(\varepsilon^{\gamma})), \quad (15)$$

where $u(\mathbf{x}_1, t) = \int_S p(\mathbf{x}_1, t, \theta_1) d\theta_1$ and $w(\mathbf{x}_1, t) = \int_S \theta_1 p(\mathbf{x}_1, t, \theta_1) d\theta_1$.

Substituting (15) into (14) and integrating with respect to θ_1, we obtain the conservation law for the macroscopic density:

$$\partial_t u(\mathbf{x}_1, t) + 2c_0 \nabla \cdot w(\mathbf{x}_1, t) = 0 \ . \qquad (16)$$

Note that the term (I) vanishes due to the symmetry in θ_1 and θ_2.

The final step is to compute the mean direction of motion w and substitute it into the conservation equation. This was done in detail in [26].

The key step of the derivation is to rewrite the collision term (I) as [26] and to use the molecular chaos assumption for low density of robots [28] given by $\tilde{\tilde{\sigma}}(\mathbf{x}_1, \mathbf{x}_1 \pm \varepsilon^{\xi}\nu, t, \theta_1, \theta_2) = p(\mathbf{x}_1, t, \theta_1) p(\mathbf{x}_1, t, \theta_2) + \mathcal{O}(\varepsilon^{\xi})$. Finally, for the term (II) we use a quasi-static approximation such that $\mathcal{B}^{\varepsilon}(\mathbf{x}_1, \varepsilon\lambda + \varepsilon^{1-\gamma} c_0 \theta_1 \cdot \nabla) \simeq \mathcal{B}^{\varepsilon}(\mathbf{x}_1, \varepsilon^{1-\gamma} c_0 \theta_1 \cdot \nabla)$, since $\gamma > 0$. Multiplying (14) by θ_1 and integrating we obtain the Theorem 1, after choosing the appropriate scaling.

VI. Robot simulations

A Lévy search strategy was implemented for the *e-puck* [37] robot, shown in Figure 1, using the Webots [36] 2019a simulator in a arena of dimensions 220cm by 180cm. Each *e-puck* is a differential wheeled robot with a circular body with a diameter of 7.5cm and 2 wheels of a diameter of 4.1cm. The robots are initially placed at centre of the simulated arena. Specifically, they are placed in a ring and oriented to face away from one another. For experiments of robot population sizes 5,10,15 and 20 the sizes of this ring are 25cm, 30cm, 40cm and 55cm.

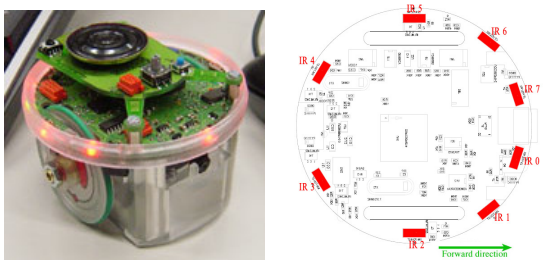

(a) (b)

Figure 1. In (a), a photograph of the real *e-puck* robot [54]. In (b), a diagram showing the placement of the *e-puck* robot's 8 Infrared proximity sensors which are used in the simulations for obstacle avoidance [55].

To track the coverage of the simulated arena, we discretized the environment by overlaying a virtual grid of 1cm×1cm cells onto it. Each cell captures the simulation time at which it was reached by any robot (hit time) and therefore the coverage at any one time can be computed by simply counting the number of non-empty cells. Figure 3 shows the simulator's display tool used to visualize visited cells (in white) and empty cells (in black).

The coverage grid is maintained by a supervisor agent within the simulation, which is able to access the position of all robots at each step of the simulation. The supervisor records these position into the coverage grid. In addition it regularly computes and saves the current coverage value.

The supervisor computes the coverage as follows [17]:

$$\text{Coverage} = \frac{\text{number of explored cells}}{\text{total number of cells}} \ . \qquad (17)$$

The controller used by each *e-puck* robots is shown in Algorithm 1[2].

The robots alternate on-the-spot turns (with rotational velocity fixed at 0.858 rad/sec) with straight movements (at 6.44

[2]Code available at https://github.com/alaromeny/epuckLevyStrategies.git

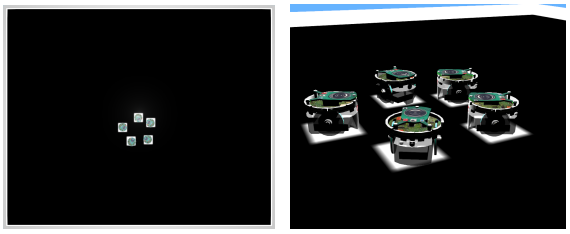

(a) (b)

Figure 2. These two images show the placement of the *e-puck* robots within the arena for all experiments with 5 robots in the Webots [36] simulator. In (a), a birds-eye view of the initial positions around the centre of the arena can be seen - the robots are placed in a ring formation. In (b), a zoomed in side view of the initial orientations in the same arena - the robots are facing away from each other.

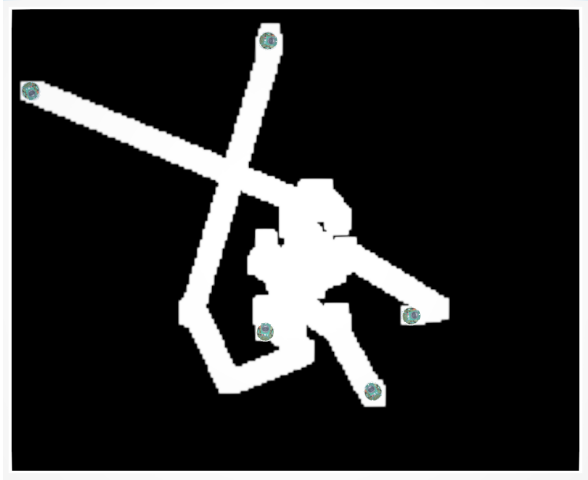

Figure 3. This image shows a birds-eye view of the coverage trails left by 5 *e-puck* robots within the arena in the Webots [36] simulator after two minutes of execution. The *e-puck* robot's (small green disk) coverage can be visualised by overlaying an image onto the base of the arena. It can be seen that the robots have left a cluster of small trails around their initial centre positions, seen in Figure 2, before performing slightly larger movements which have spread the robots out within the area.

```
while True do
    (x_new, y_new) = lévyDistribution()
    distanceToTravel = norm((x_new, y_new))
    angle = atan2((x_new, y_new))
    rotateRobot(angle)
    while distanceTraveled < distanceToTravel do
        if no obstacles are detected then
            moveForward()
        else
            break
        end
    end
end
```

Algorithm 1: *e-puck* Lévy Search controller. This algorithm outlines the behaviour of the *e-puck* robots. The robot's new position is calculated within the `lévyDistribution()` function and calculations required for this are shown in (18).

cm/sec) in the direction of target points that are computed using the Lévy distribution relative to their current position. The robots stop and compute a new target point whenever their on-board Infrared (IR) range sensors detect an obstacle (either another robot or the borders of the arena).

The movement of each *e-puck* is characterized by long distance runs, where the run distance r is generated from a Lévy process [31]

$$r = \frac{\sin((\mu-1)\tilde{X}_1)}{\cos(\tilde{X}_1)^{1/\mu-1}}\left(\frac{\cos((2-\mu)\tilde{X}_1)}{\tilde{X}_2}\right)^{\frac{2-\mu}{\mu-1}}, \qquad (18)$$

and the new positions are computed, for $\theta = \pi X_3$, as

$$x_{\text{new}} - x_{\text{current}} = r\cos(\theta), \text{ and } y_{\text{new}} - y_{\text{current}} = r\sin(\theta)\,. \quad (19)$$

Here, the parameter $\mu \in (1,3)$, $\tilde{X}_1 = {}^1\!/\!_\pi X_1$ is a uniform random variable in the interval $[-{}^\pi\!/\!_2,\ {}^\pi\!/\!_2]$, $\tilde{X}_2 = -\ln X_2$ has a unit exponential distribution and $X_1 = X_2 = X_3$ are uniformly distributed random variables in the interval $(0,1)$. Since we are calculating the new location (x,y) relative to the base of the robot, we can set $x_{\text{current}} = y_{\text{current}} = 0$.

Each experiment is run for $T = 20$ minutes and coverage values are recorded every second. The supervisor agent then resets the robots into their original positions, clears the coverage grid and saves experiment data to a file. These experiments are run in batches so that data for hundreds of different runs can be captured and compared. Experiments were run for different parameters; $N = 5, 10, 15, 20$; and $\mu = 2.1, 2.3, 2.5, 2.7, 2.9$. Note that $\alpha = \mu - 1$ in the rest of the paper.

VII. Optimal Control and Numerical Implementation

We briefly discuss how to use the continuum descriptions in this paper towards the development of optimal search and targeting strategies for swarm robotic systems. We present an optimal control approach to compute controls and parameters from the continuum model in an efficient manner. Further details on optimal control may be found in [49].

One is often interested in achieving a desired task $G(x,t)$ in an optimal manner. This results in a general optimal control problem given by the following functional $\hat{J}(u,y,G(x,t))$:

$$\min_{(u,y)\in H\times Y} \hat{J}(u,y,G(x,t)),$$

subject to the equation (1), where H, Y are the Bochner spaces $L^2(0,T;X)$, with X a Banach space. We seek a control $y \in Y$ such that a given cost functional is optimized with respect to the given task $G(x,t)$ and state u. Tasks of interest in the case of swarm robotic systems include surveillance, optimal search strategies or optimal strategies for coverage. We illustrate this for a problem of optimal coverage.

The optimal control of the coverage problem is given by a cost functional $J(u,y)$ involving the coverage defined in (4). In its computationally efficient relaxation, related to [5], we seek $(u,y) \in H \times Y$ which minimizes

$$J(u,y) = \frac{1}{2}\|u(\cdot,T) - \mathbf{U}\|^2_{L^2(\Omega)} + \frac{\lambda}{2}\|y\|^2_{L^2(0,T;L^2(\Omega))}, \quad (20)$$

subject to equation (1) with constant $F(u)$ and Neumann boundary conditions:

$$\partial_t u - c_0 \nabla^{\alpha-1} \cdot (\widetilde{C}_\alpha \nabla u) = y \tag{21}$$
$$u(x,0) = u_0 \tag{22}$$
$$\mathcal{N}_\alpha u = 0. \tag{23}$$

Here $\mathbf{U}$ is the uniform distribution and $\mathcal{N}_\alpha u$ is the nonlocal normal derivative defined in [15]. The relaxed problem is posed in $X = L^2(\Omega)$, hence $H = L^2(0,T;L^2(\Omega))$, and Y is the set of admissible control inputs such that

$$Y = \{y \in L^2(0,T,L^2(\Omega)) : y_{min}(x,t) \le y(x,t) \le y_{max}(x,t) \quad \forall t \in (0,T),\ \forall x \in \Omega\}.$$

The upper and lower bounds y_{min}, y_{max} of the control are given by the physical parameters of the experiments.

The adjoint equation of state for the equation (21) with respect to the functional J is given by:

$$-\partial_t w - c_0 \nabla^{\alpha-1} \cdot (\widetilde{C}_\alpha \nabla w) = 0,$$
$$w(T) = u(\cdot,T) - \mathbf{U},$$
$$\mathcal{N}_\alpha w = 0.$$

Numerical simulations of (21) are based on a finite element approximation of the nonlocal partial differential equation, see [1]. We consider the weak formulation

$$\int_0^T \langle \partial_t u, v\rangle - \langle c_0 \widetilde{C}_\alpha \nabla^{\alpha-1} u, \nabla v\rangle dt = \int_0^T \langle y, v\rangle dt - \langle u_0, v(0)\rangle, \tag{24}$$

for $u, v \in W(0,T) = \{v \in L^2(0,T;H^s(\Omega)) : \partial_t v \in L^2(0,T;H^{-s}(\Omega))\}$ where $H^s(\Omega)$ is a Sobolev space of smoothness s. The bilinear form $\langle \nabla^{\alpha-1} u, \nabla v\rangle$ is implemented using quadrature methods commonly used for singular integral operators [1], [30].
The fully discrete time stepping scheme reads as follows: Find $\{u_h^1, u_h^2, \dots\} \in W_h(0,T)$ such that

$$(M - \triangle t\ A)\, u_h^{n+1} = M\ u_h^n + \triangle t\ \mathbf{b}^n,$$

where u_h^0 is given. $M,\ A$ are the mass and stiffness matrices related to the piecewise linear basis functions ϕ_i of H_h defined by $M_{ij} = (\phi_i, \phi_j)$, $A_{ij} = \langle \nabla^{\alpha-1}\phi_i, \nabla\phi_j\rangle$, and $\mathbf{b}^n$ is the Galerkin projection of y onto $W_h(0,T)$ at time step n.
The weak formulation of the adjoint problem is similar and reads as follows:

$$\int_0^T -\langle \partial_t w, v\rangle - \langle c_0 \widetilde{C}_\alpha \nabla w, \nabla^{\alpha-1} v\rangle dt = \langle w(T), v(T)\rangle. \tag{25}$$

It is discretised in the same way as the forward problem.

VIII. Comparison between macroscopic model and individual robot simulations

For the numerical experiments we consider a robotics arena given by $\Omega = [-0.9, 0.9] \times [-1.1, 1.1]$ to match the webots simulation. The initial condition for the continuum model (1) is $u_0(x) = \max\left(0, 1.2\exp\frac{-4N|x|^2}{0.075} - 0.2\right)$. It approximates the initial condition for the individual *e-puck* webots simulations described in Section VI.

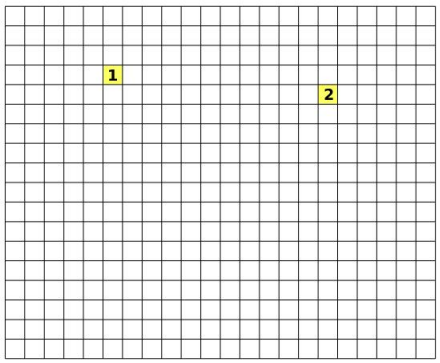

Figure 4. Domain for macroscopic simulation as well as webots individual particle simulation. Tiles 1 and 2 are highlighted for convenience later.

From the physical characteristics of the robots described in Section VI, we obtain the scaling parameters, $\varepsilon = 0.005$, $c_n = 3,\ \gamma = 1/2,\ c_0 = 3 \cdot 0.005^\gamma$, in Section V-B.

Figure 5 compares PDE and webots individual agent simulations for different numbers of robots, $N = 5,\ 10,\ 15,\ 20$ for a Lévy exponent $\alpha = 1.3$. The coverage increases with time and N, and the average of the webots simulations agrees closely with the PDE solution. Figure 6 similarly compares the coverage as a function of α, with $N = 20$, and finds close agreement between the PDE simulations and the average of webots simulations. We note that coverage increases with decreasing α, showing the advantage of long-range Lévy strategies.
In all cases, as the number of robots N increases we observe an increase in coverage efficiency as well as a decrease in the variation of the individual runs. In the transient regime far from full coverage, the variations are significantly larger for the longer-ranged Lévy strategies.

Figure 7 compares the average time to reach a coverage of 50% for various values of α for $N = 20$ robots. Note that the average time increases when α increases. The macroscopic simulation falls within one standard deviation from the webots individual agent simulations, justifying the statistical significance of the results.

In Figure 8 we compare the coverage of the webots simulations with $N = 20$ against the continuous model for different values of α at the final time $T = 1200s$. Note that the continuous model falls within one standard deviation from the individual robot simulation and exhibits a decreasing trend of coverage as a function of α.
Figure 9 illustrates the hitting time efficiency for different values of α at $T = 1200s$ for $N = 5$ robots based on the individual particle simulations. We note that as the value of α increases the hitting time of each tile increases. In particular,

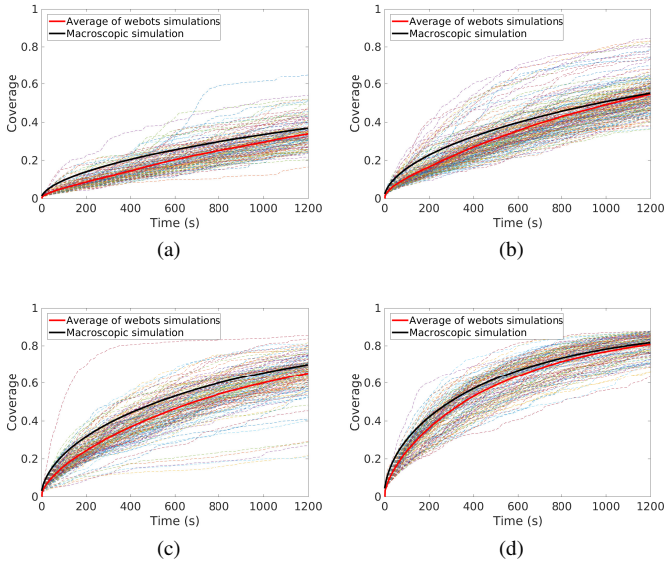

Figure 5. Comparison of the webots simulations with the macroscopic model for $\alpha = 1.3$ and varied number of robots $N = 5, 10, 15, 20$.

for values of α close to 2, a significant part of the arena remains to be covered, as shown in black. As the value of α approaches 1 large expected hitting times (in yellow) are only observed close to the boundary of the domain. This again underlines the advantage of long-range Lévy strategies for efficient coverage.

Figure 10 shows the increase in the average hitting time for different values of α for two fixed tiles sized $10 \times 10cm$ in the arena, centered at $(-0.55, 0.55)$, respectively $(0.55, 0.45)$ as highlighted in Figure 4. Curves for tile 1 and tile 2 are generated from average of 70 runs for each value of α. The webots simulations are compared to the macroscopic model as well as the analytic approximation of the hitting times given by the following explicit formula obtained in [27]:

$$t_0 \simeq \frac{\delta\pi}{2^\alpha \hat{C}_\alpha \, \mathrm{vol}(\mathsf{T}) \sum_i |\mathbf{x}_0 - \mathbf{x}_i|^{-\alpha-2}} \, . \qquad (26)$$

Here $\mathbf{x}_0$ is the centre of the target T, $\mathbf{x}_i$ corresponds to the initial positions of the robots and $\hat{C}_\alpha = \Xi_\alpha C_\alpha$ from Appendix A. The target T is considered to be covered when the solution reaches a prescribed threshold $\delta \in (0, 1)$.
Note that the analytic approximation closely matches both the macroscopic and the individual agent simulations.

The favorable long-range behaviour of Lévy over Brownian strategies is shown by the increase in coverage for smaller values of α. This is illustrated by the clear quantitative agreement of macroscopic modelling and webots individual particle simulations which falls within one standard deviation of the statistical uncertainty.

In all simulations, the macroscopic modelling is faster and more efficient by orders of magnitude, at least 100, and the numerical results confirm the proposed definitions of coverage and hitting times. The efficient computation of these quantities is crucial for real-time optimization of robot movement strategies.

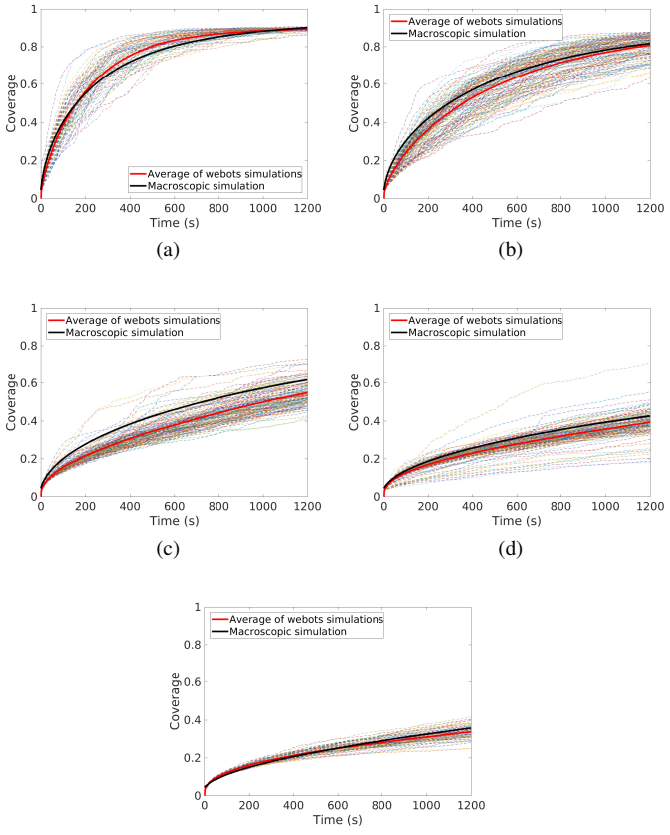

Figure 6. Comparison of the webots simulation with the macroscopic model for $N = 20$ and various $\alpha = 1.1,\ 1.3,\ 1.5,\ 1.7,\ 1.9$.

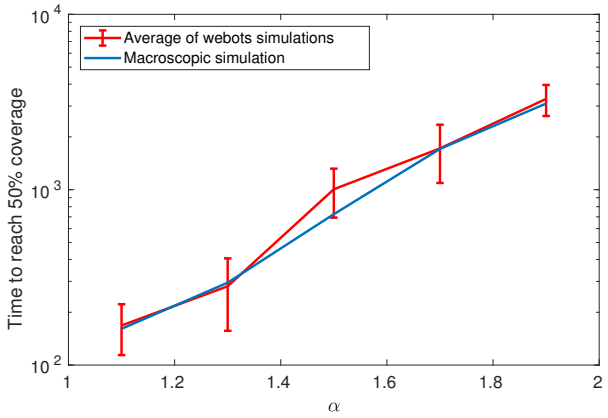

Figure 7. Comparison of average time to reach 50% coverage for various values of α and $N = 20$ robots.

We note that statistical deviations are larger for small number of robots, where also larger finite size effects are expected to play a role for the macroscopic models as can be seen in Figure 5. During intermediate times, statistical deviations are observed to be larger for small Lévy parameters α. On the other hand, statistical certainty increases for longer

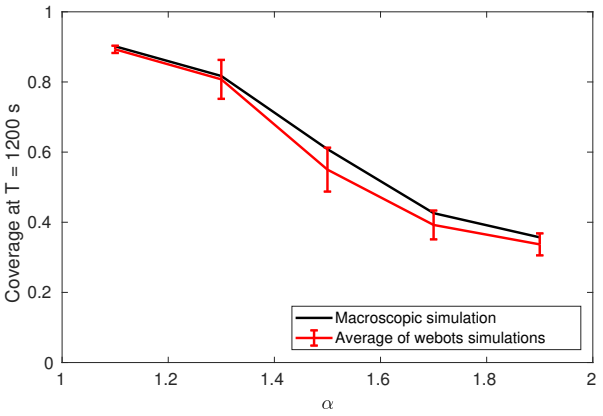

Figure 8. Comparison of coverage efficiency as a function of α for $N = 20$ robots at $T = 1200s$.

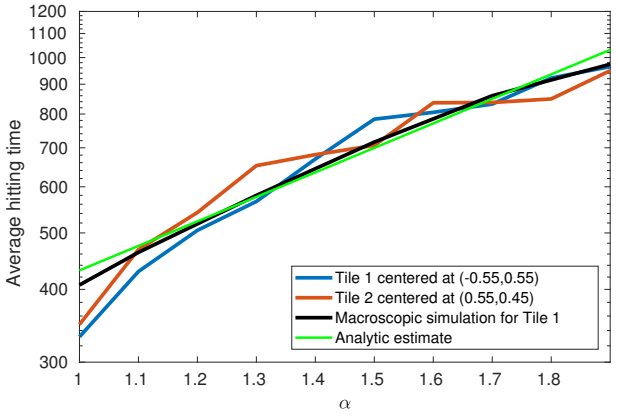

Figure 10. Hitting times with $N = 5$ robots for two tiles in the domain centered at $(-0.55, 0.55)$ and $(0.55, 0.45)$, compared to the analytic solution in (26).

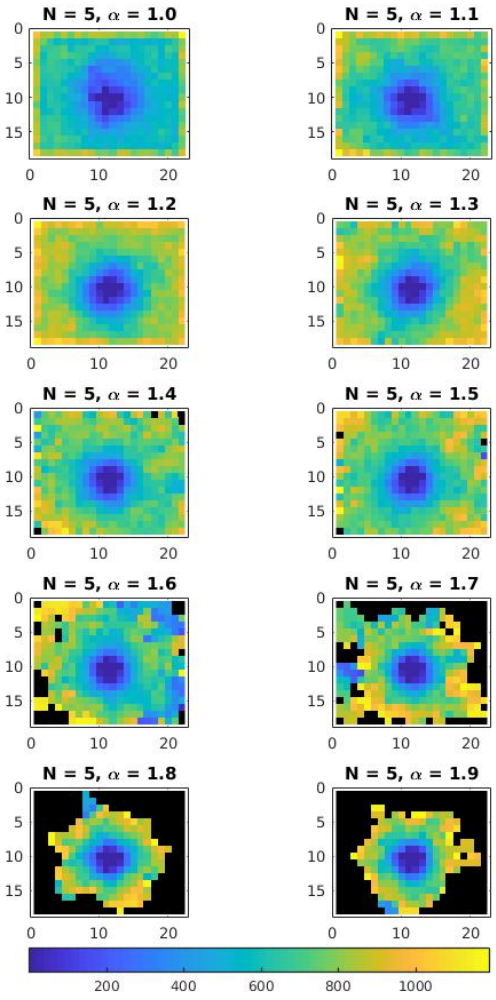

Figure 9. Expected hitting times taken from the webots simulation at $T = 1200s$ for $N = 5$ and different α. Yellow colour corresponds to higher hitting times, blue corresponds to lower hitting times.

times for values near full coverage. This is illustrated in Figure 8 for which the error bars are largest for intermediate values of α.

IX. Conclusions

In this paper we show the opportunities provided by *analysis tools* developed for biological systems, like macroscopic modelling, for the assessment and design of swarm robotic systems. We illustrate our approach on automated search and area coverage applications. Starting from the behaviour of the individual robot, these tools allow the fast quantitative prediction of system-level properties and thereby provide a way towards the optimal engineering of a system for a given task, including qualitative analytical methods.

From the movement and interaction strategies of the individual robots we derive an effective diffusion equation for the density of robots on macroscopic length and time scales. We do so for a large class of Lévy strategies with characteristic long-range movement and compare it to regular diffusive strategies. The effective description allows the fast and accurate computation of quantities of robotic interest: We show that coverage and expected hitting times agree with the results of standard individual robot simulations within the statistical error margins of the latter, at less than 1% of the computational cost. We confirm that Lévy strategies outperform regular diffusion. The results underline the exponential increase of the hitting time with the Lévy exponent, for constant robot speed, with matching analytical and numerical results.

For a given metric to be optimized in a specific problem, we formulate a control problem to compute the optimal parameters for the macroscopic equation, which translate into a strategy for the individual robots. Our macroscopic approach provides a way to overcome the computational limitations of particle simulations in the design of swarm robotic systems. Work in [5], [7] has started to investigate metrics relevant to robotics applications. Also direct approaches to the control of the interacting particle system are a topic of current interest [6].

Macroscopic models by partial differential equations have become a standard modelling tool in biological contexts [9], [19]. Future work aims to adapt the available tool box towards other swarm robotics applications, including pheromone cues, long-range coordination [26], strategies for complex domains, such as exploration of unknown and hazardous environments [25], and validation with real robot systems.

APPENDIX A
DEFINITIONS OF FRACTIONAL OPERATORS

We recall some basic definitions concerning fractional differential operators, as well as their relation to the turning operator T.

Definition A.1. For $s \in (0,2)$ and $f \in C^2(\mathbb{R}^n)$ define the fractional gradient of f as

$$\nabla^s f(\mathbf{x}) = \frac{1}{|S|}\int_S \theta \mathbf{D}_\theta^s f(\mathbf{x}) d\theta = \frac{1}{|S|}\int_S \theta(\theta\cdot\nabla)^s f(\mathbf{x}) d\theta, \tag{27}$$

where $\mathbf{D}_\theta^s = (\theta\cdot\nabla)^s$ is the fractional directional derivative of order s. The fractional Laplacian of f is given by

$$\mathbb{D}^s f(\mathbf{x}) = \frac{1}{|S|}\int_S \mathbf{D}_\theta^s f(\mathbf{x}) d\theta. \tag{28}$$

$\mathbb{D}^s$ is associated to $(-\Delta)^{\alpha/2}$ as follows,

$$\mathbb{D}^s f(\mathbf{x}) = \Xi_\alpha (-\Delta)^{\alpha/2}$$

where, in two dimensions, for $1<\alpha<2$,

$$\Xi_\alpha = -2\sqrt{\pi}\cos\left(\frac{\pi\alpha}{2}\right)\frac{\Gamma\left(\frac{\alpha+1}{2}\right)}{\Gamma\left(\frac{\alpha+2}{2}\right)}. \tag{29}$$

See [35] for further information.

ACKNOWLEDGMENTS

The authors would like to thank J. A. Carrillo, K. J. Painter and H. Sardinha for fruitful discussions and H. Fraser and M. A. Campbell for technical assistance.

REFERENCES

[1] Gabriel Acosta and Juan Pablo Borthagaray. A fractional Laplace equation: regularity of solutions and finite element approximations. *SIAM Journal on Numerical Analysis*, 55(2):472–495, 2017.

[2] J. Aguilar, D. Monaenkova, V. Linevich, W. Savoie, et al. Collective clog control: Optimizing traffic flow in confined biological and robophysical excavation. *Science*, 361(6403):672–677, 2018.

[3] Wolfgang Alt. Biased random walk models for chemotaxis and related diffusion approximations. *Journal of Mathematical Biology*, 9(2):147–177, 1980.

[4] Yaniv Altshuler, Alfred M Bruckstein, and Israel A Wagner. Swarm robotics for a dynamic cleaning problem. In *Swarm intelligence in intrusion detection: A survey, 2011. Computers & Security,*, pages 209–216. IEEE, 2005.

[5] Brendon G Anderson, Eva Loeser, Marissa Gee, Fei Ren, Swagata Biswas, Olga Turanova, Matt Haberland, and Andrea L Bertozzi. Quantitative assessment of robotic swarm coverage. *arXiv preprint, arXiv:1806.02488*, 2018.

[6] Rafael Bailo, Mattia Bongini, José A. Carrillo, and Dante Kalise. Optimal consensus control of the Cucker-Smale model. *arXiv preprint, arXiv:1802.01529*, 2018.

[7] Manuele Brambilla, Eliseo Ferrante, Mauro Birattari, and Marco Dorigo. Swarm robotics: a review from the swarm engineering perspective. *Swarm Intelligence*, 7:1–41, 2013.

[8] Carlo Cercignani, Reinhard Illner, and Mario Pulvirenti. *The mathematical theory of dilute gases*, volume 106. Springer Science & Business Media, 2013.

[9] Edward A. Codling, Michael J. Plank and Simon Benhamou. Random walk models in biology. *Journal of the Royal Society Interface*, 5(25):813–834, 2008.

[10] Micael S Couceiro, Patricia A Vargas, Rui P Rocha, and Nuno MF Ferreira. Benchmark of swarm robotics distributed techniques in a search task. *Robotics and Autonomous Systems*, 62(2):200–213, 2014.

[11] Micael S. Couceiro, Patricia A. Vargas, and Rui P. Rocha. Bridging the reality gap between the webots simulator and e-puck robots. *Robotics and Autonomous Systems*, 62(10):1549 – 1567, 2014.

[12] Iain D. Couzin, Jens Krause, Richard James, Graeme D. Ruxton and Nigel R. Franks. Collective memory and spatial sorting in animal groups. *Journal of Theoretical Biology*, 218(1):1–11, 2002.

[13] Pierre Degond and Sébastien Motsch. Continuum limit of self-driven particles with orientation interaction. *Mathematical Models and Methods in Applied Sciences*, 18(supp01):1193–1215, 2008.

[14] Amit Dhariwal, Gaurav S Sukhatme, and Aristides AG Requicha. Bacterium-inspired robots for environmental monitoring. In *Robotics and Automation, 2004. Proceedings. ICRA'04. 2004 IEEE International Conference*, 1436–1443. IEEE, 2004.

[15] Serena Dipierro, Xavier Ros-Oton, and Enrico Valdinoci. Nonlocal problems with Neumann boundary conditions. In *Revista Matematica Iberoamericana* 33 (2017), 377-416.

[16] Marco Dorigo, Mauro Birattari, and Manuele Brambilla. Swarm robotics. *Scholarpedia*, 9(1):1463, 2014.

[17] Filip Fossum, Jean-Marc Montanier, and Pauline C. Haddow. Repellent pheromones for effective swarm robot search in unknown environments. In *2014 IEEE Symposium on Swarm Intelligence (SIS)* 1-8. IEEE, 2014

[18] Jakob Fredslund and Maja J Mataric. Robot formations using only local sensing and control. In *Computational Intelligence in Robotics and Automation, 2001. Proceedings 2001 IEEE International Symposium on*, pages 308–313. IEEE, 2001.

[19] Thomas Hillen and Kevin J. Painter. A user's guide to PDE models for chemotaxis. *Journal of Mathematical Biology*, 58(1–2):183, 2009.

[20] George Kantor, Sanjiv Singh, Ronald Peterson, Daniela Rus, Aveek Das, Vijay Kumar, Guilherme Pereira, and John Spletzer. Distributed search and rescue with robot and sensor teams. In *Field and Service Robotics*, pages 529–538. Springer, 2003.

[21] Constantinos Kolias, Georgios Kambourakis, and M Maragoudakis. Swarm intelligence in intrusion detection: A survey. *Computers & Security*, 30(8):625–642, 2011.

[22] M. Krivonosov, S. Denisov, V. Zaburdaev. Lévy robotics. *arXiv*, 1612.03997, 2016.

[23] Wenguo Liu, Alan FT Winfield, and Jin Sa. Modelling swarm robotic systems: A case study in collective foraging. *Towards Autonomous Robotic Systems*, pages 25–32, 2007.

[24] K. Elamvazhuthi and S. Berman. Optimal control of stochastic coverage strategies for robotic swarms. In *2015 IEEE International Conference on Robotics and Automation (ICRA)*, pages 1822–1829, May 2015.

[25] Gissell Estrada-Rodriguez, Ernesto Estrada and Heiko Gimperlein. Metaplex networks: Influence of the exo-endo structure of complex systems on diffusion. *arXiv preprint, arXiv:1812.11615*, 2018.

[26] Gissell Estrada-Rodriguez and Heiko Gimperlein. Swarming of interacting robots with Lévy strategies: a macroscopic description. *arXiv preprint, arXiv:1807.10124*, 2018.

[27] Gissell Estrada-Rodriguez, Heiko Gimperlein, Kevin J. Painter, and Jakub Stocek. Space-time fractional diffusion in cell movement models with delay. *Mathematical Models and Methods in Applied Sciences*, 29, pages 65–88, 2019.

[28] Benjamin Franz, Jake P Taylor-King, Christian Yates, and Radek Erban. Hard-sphere interactions in velocity-jump models. *Physical Review E*, 94(1):012129, 2016.

[29] George Matthew Fricke, Joshua P. Hecker, Judy L. Cannon, and Melanie E. Moses. Immune-inspired search strategies for robot swarms. *Robotica*, 34(8):1791–1810, 2016.

[30] Heiko Gimperlein and Jakub Stocek. Space-time adaptive finite elements for nonlocal parabolic variational inequalities. *arXiv preprint, arXiv:1810.06888*, 2018.

[31] Tajie Harris et al. Generalized Lévy walks and the role of chemokines in migration of effector CD8+ T cells. *Nature*, pages 545–548, volume 486, 2012.

[32] Earle Hess Kennard et al. *Kinetic theory of gases, with an introduction to statistical mechanics*. McGraw-Hill, 1938., 1938.

[33] Ali Marjovi, João Gonçalo Nunes, Lino Marques, and Aníbal de Almeida. Multi-robot exploration and fire searching. In *Intelligent Robots and Systems, 2009. IROS 2009. IEEE/RSJ International Conference on*, pages 1929–1934. IEEE, 2009.

[34] Maja J Matarić. Reinforcement learning in the multi-robot domain. In *Robot colonies*, pages 73–83. Springer, 1997.

[35] Mark M. Meerschaert, Jeff Mortensen and Stephen W. Wheatcraft Fractional vector calculus for fractional advection–dispersion. *Physica A: Statistical Mechanics and its Applications*, 367:181–190, 2006.

[36] Olivier Michel. Cyberbotics Ltd. webots™: professional mobile robot simulation. *International Journal of Advanced Robotic Systems*, 1(1):5, 2004.

[37] F. Mondada and et al. The e-puck, a robot designed for education in engineering. In *Proceedings of the 9th Conference on Autonomous Robot Systems and Competitions*, pages 59–65, 2009.

[38] Stefano Nolfi and Dario Floreano. *Evolutionary robotics: The biology, intelligence, and technology of self-organizing machines*. MIT press, 2000.

[39] Kristina Lerman, Alcherio Martinoli and Aram Galstyan. A review of probabilistic macroscopic models for swarm robotic systems *International Workshop on Swarm Robotics*, pages 143–152, 2004.

[40] Surya G. Nurzaman, Yoshio Matsumoto, Yutaka Nakamura, Satoshi Koizumi and Hiroshi Ishiguro. Yuragi-based adaptive searching behavior in mobile robot: From bacterial chemotaxis to Levy walk. *Robotics and Biomimetics, 2008. ROBIO 2008. IEEE International Conference on*, 806–811, 2009.

[41] Hans G Othmer and Thomas Hillen. The diffusion limit of transport equations derived from velocity-jump processes. *SIAM Journal on Applied Mathematics*, 61(3):751–775, 2000.

[42] Lynne E Parker. On the design of behavior-based multi-robot teams. *Advanced Robotics*, 10(6):547–578, 1995.

[43] Lynne E Parker. Distributed intelligence: Overview of the field and its application in multi-robot systems. *Journal of Physical Agents*, 2(1):5–14, 2008.

[44] Erol Şahin, Sertan Girgin, Levent Bayindir, and Ali Emre Turgut. Swarm robotics. In *Swarm intelligence*, pages 87–100. Springer, 2008.

[45] Thomas Schmickl, Ronald Thenius, Christoph Moslinger, Jon Timmis, Andy Tyrrell, Mark Read, James Hilder, Jose Halloy, Alexandre Campo, Cesare Stefanini, et al. Cocoro–the self-aware underwater swarm. In *Self-Adaptive and Self-Organizing Systems Workshops (SASOW), 2011 Fifth IEEE Conference on*, pages 120–126. IEEE, 2011.

[46] Madhubhashi Senanayake, Ilankaikone Senthooran, Jan Carlo Barca, Hoam Chung, Joarder Kamruzzaman, and Manzur Murshed. Search and tracking algorithms for swarms of robots: A survey. *Robotics and Autonomous Systems*, 75:422–434, 2016.

[47] Donny Sutantyo, Paul Levi, Christoph Möslinger and Mark Read. Collective-adaptive Lévy flight for underwater multi-robot exploration. *2013 IEEE International Conference on Mechatronics and Automation (ICMA)*, 456–462, 2013.

[48] Jake P. Taylor-King, Benjamin Franz, Christian A Yates, and Radek Erban. Mathematical modelling of turning delays in swarm robotics. *IMA Journal of Applied Mathematics*, 80(5):1454–1474, 2015.

[49] Fredi Tröltzsch. Optimal Control of Partial Differential Equations: Theory, Methods, and Applications. *American Mathematical Society*, 112, 2010.

[50] Mirbek Turduev, Murat Kirtay, Pedro Sousa, Veysel Gazi, and Lino Marques. Chemical concentration map building through bacterial foraging optimization based search algorithm by mobile robots. In: *Systems Man and Cybernetics (SMC), 2010 IEEE International Conference*, pages 3242–3249. IEEE, 2010.

[51] Patricia A. Vargas, Ezequiel A. Di Paolo, Inman Harvey and Phil Husbands. The Horizons of Evolutionary Robotics. *The MIT Press*, 1st, 2015.

[52] Tamás Vicsek, András Czirók, Eshel Ben-Jacob, Inon Cohen and Ofer Shochet. Novel type of phase transition in a system of self-driven particles. *Physical Review Letters*, 75(6):1226, 1995.

[53] Fangbo Zhang, Andrea L Bertozzi, Karthik Elamvazhuthi, and Spring Berman. Performance bounds on spatial coverage tasks by stochastic robotic swarms. *IEEE Transactions on Automatic Control*, 63(6):1563–1578, 2018.

[54] GCTronic. e-puck education robot - an overview. http://www.e-puck.org/. (Accessed on 03/01/2019).

[55] GCTronic. epuck robot with proximity sensors description. http://www.e-puck.org/index.php?option=com_content&view=article&id=22&Itemid=13. (Accessed on 03/01/2019).

Siobhan Duncan received both her BEng in Computing and Electronics and MRes in Robotics and Autonomous Systems from Heriot-Watt University in Edinburgh, U.K. She is currently working towards her PhD within the Edinburgh Centre for Robotics in Edinburgh, U.K. Her current research interest focuses on stigmergy applied to swarm robotics and how this can be integrated with modern technologies such as IoT and Cloud Computing to help bring swarm robotics into field application. In addition to her academic work, she is interested in widening access to robotics in particular for women and girls, children from SIMD areas and those living in isolated rural communities in Scotland.

Gissell Estrada-Rodriguez received the BSc degree in mathematics and physics from Strathclyde University, Glasgow, U.K. in 2015. She is currently working towards the Ph.D. degree in mathematics with the Maxwell Institute Graduate School of Analysis and its Applications, Edinburgh, U.K. Her research interests are focused on the derivation, analysis and numerical analysis of partial differential equations for biological and robotics systems.

Jakub Stocek received the BSc degree in mathematics from Heriot-Watt University, Edinburgh, U.K. in 2016. He is currently working towards the Ph.D. degree in mathematics with the Maxwell Institute Graduate School of Analysis and its Applications, Edinburgh, U.K. His research interests are focused on numerical analysis and applications of partial differential equations and nonlocal operators.

Mauro Dragone is Assistant Professor with the School of Engineering & Physical Sciences; Sensors, Signals & Systems at Heriot-Watt University, Edinburgh, UK. His research expertise includes Cognitive Robotics, Human-Robot Interaction, Wireless Sensor Networks, Multiagent Systems and Internet of Things.

Patricia A. Vargas received her Ph.D. in Computer Engineering from the University of Campinas, Unicamp (Brazil) in 2005. She is currently Director of the Robotics Laboratory and Associate Professor in Computer Science and Robotics at the School of Mathematical and Computer Science at Heriot-Watt University (Edinburgh, Scotland, UK). She was a post-doc at the Centre for Computational Neuroscience and Robotics, University of Sussex (England, UK) for 3 years. Her research interests include evolutionary and bio-inspired robotics, swarm robotics, computational neuroscience, data mining and machine learning, biologically-inspired algorithms and human–robot interaction.

Heiko Gimperlein received the M.Sc. degrees in physics and in mathematics and a Ph.D. degree in mathematics from Leibniz University Hannover, Germany, in 2006 and 2010, respectively.

From 2010 to 2013 he was a Postdoctoral Researcher in the Department of Mathematics at the University of Copenhagen, Denmark. Since 2013 he has been at Heriot-Watt University, Edinburgh, UK, currently as Associate Professor. His research interests include mathematical analysis and its applications to engineering and the natural sciences.